Editors' Suggestion

Conclusive Experimental Demonstration of One-Way Einstein-Podolsky-Rosen Steering

Nora Tischler,[1] Farzad Ghafari,[1] Travis J. Baker,[1] Sergei Slussarenko,[1] Raj B. Patel,[1,2] Morgan M. Weston,[1] Sabine Wollmann,[1,3] Lynden K. Shalm,[4] Varun B. Verma,[4] Sae Woo Nam,[4] H. Chau Nguyen,[5] Howard M. Wiseman,[1] and Geoff J. Pryde[1,*]

[1]*Centre for Quantum Computation and Communication Technology (Australian Research Council), Centre for Quantum Dynamics, Griffith University, Brisbane, Queensland 4111, Australia*

[2]*Centre for Quantum Computation and Communication Technology (Australian Research Council), Quantum Photonics Laboratory, School of Engineering, RMIT University, Melbourne, Victoria 3000, Australia*

[3]*Quantum Engineering Technology Labs, H. H. Wills Physics Laboratory and Department of Electrical and Electronic Engineering, University of Bristol, Bristol BS8 1FD, United Kingdom*

[4]*National Institute of Standards and Technology, 325 Broadway, Boulder, Colorado 80305, USA*

[5]*Naturwissenschaftlich-Technische Fakultät, Universität Siegen, Walter-Flex-Straße 3, D-57068 Siegen, Germany*

(Received 31 May 2018; revised manuscript received 2 August 2018; published 7 September 2018)

Einstein-Podolsky-Rosen steering is a quantum phenomenon wherein one party influences, or steers, the state of a distant party's particle beyond what could be achieved with a separable state, by making measurements on one-half of an entangled state. This type of quantum nonlocality stands out through its asymmetric setting and even allows for cases where one party can steer the other but where the reverse is not true. A series of experiments have demonstrated one-way steering in the past, but all were based on significant limiting assumptions. These consisted either of restrictions on the type of allowed measurements or of assumptions about the quantum state at hand, by mapping to a specific family of states and analyzing the ideal target state rather than the real experimental state. Here, we present the first experimental demonstration of one-way steering free of such assumptions. We achieve this using a new sufficient condition for nonsteerability and, although not required by our analysis, using a novel source of extremely high-quality photonic Werner states.

DOI: 10.1103/PhysRevLett.121.100401

Introduction.—One of the most noteworthy and fundamental features of quantum mechanics is the fact that it admits stronger correlations between distant objects than what would be possible in a classical world. Quantum correlations can be categorized into the following classes, which form a strict hierarchy [1–3]: Entanglement is a superset of Einstein-Podolsky-Rosen (EPR) steerability, which, in turn, is a superset of Bell nonlocality. Out of these, steering is special in that it allows for, and, in fact, intrinsically contains, asymmetry. Steering is operationally defined as a quantum information task, where one untrusted party (for instance, called Alice) tries to convince another distant, trusted party (Bob) that they share entanglement. Bob asks Alice to make certain measurements on her quantum system (e.g., particle) and to announce the measurement outcomes but is not sure whether Alice answers honestly or indeed even has a particle. He also makes corresponding measurements on his particle and checks whether the correlations of their measurement outcomes rule out a so-called local hidden state model for his particle, thereby proving shared entanglement [1].

Interestingly, the steering task allows for the case of one-way steerable states, for which steering is possible in one direction but impossible in the reverse direction [4]. One-way steering is of foundational interest, since it is a striking manifestation of asymmetry that does not exist for entanglement and Bell nonlocality. It also has applications in device-independent quantum key distribution [5]. To observe one-way steering, one needs to demonstrate steering in one direction, by violating a steering inequality. In addition, one must establish that it would be impossible to achieve steering in the opposite direction. Our scheme, which allows for arbitrary measurements and rigorously takes into account losses and the real experimental quantum state, is illustrated in Fig. 1.

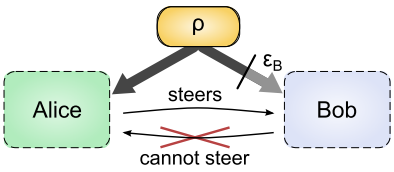

FIG. 1. Scheme for demonstrating one-way steering. A two-qubit quantum state is distributed to Alice and Bob, with a lossy channel on the way to Bob, such that his probability of obtaining his qubit is ε_B. A detection-loophole-free steering test demonstrates that Alice can steer Bob's state. At the same time, it is established that Bob cannot steer Alice's state for any choice of measurements, based directly on the reconstructed experimental quantum state ρ and the measured efficiency ε_B.

Since the question of whether one-way steering is possible was first raised in the seminal paper of Ref. [1], considerable progress has been made on the topic [2,4,6–17]. First, the original question was answered in the affirmative, and this gave rise to the quest to fully understand and demonstrate the phenomenon. An overarching effort of these works has been the elimination of assumptions.

On the theory side, the ultimate, so far unattained, goal would be to establish practical necessary and sufficient conditions for the steerability of arbitrary quantum states using arbitrary measurements, which are described by positive operator-valued measures (POVMs). Examples of one-way steerable states have been identified assuming projective measurements [4,9,11] and for POVMs [2,8,10]. While specific example states provide conclusive proof that one-way steering is possible in principle, they are challenging to work with in real experiments. Real states in the laboratory generally deviate from the ideal target states, so the ability to account for these deviations is crucial. A practical, sufficient condition for the nonsteerability of arbitrary two-qubit states under the assumption of projective measurements is known [11]. Recently, a practical, sufficient condition for the nonsteerability of generic two-qubit states with loss was also established for restricted projective measurements [17] (see explanation in Supplemental Material, Sec. I [18]).

The elimination of assumptions has also been a key development on the experimental side. Several experiments relied on assumptions about the measurements. The first demonstration of one-way steering was restricted to the case of Gaussian measurements [7]. This was followed by a demonstration that was restricted to two-setting projective measurements [12] and another one assuming multisetting projective measurements [14]. In contrast to these post-selection-based experiments, an experiment by some of us and co-workers had no detection loophole, and, therefore, its analysis could take into account vacuum state contributions to the quantum state [10]. Also, unlike the previous experiments, it made no assumptions about the measurement. It did, however, make an assumption about the type of quantum state; an analysis for Werner states was applied to the experimentally achieved state, which exhibited a high fidelity with a Werner state. However, drawing conclusions based on high fidelities can be problematic, in general [21], and caution is also warranted for the case at hand [17] (see also Sec. V in Ref. [18]).

Here, we present the first fully rigorous experimental demonstration of two-qubit one-way steering. In one direction, we demonstrate the violation of a steering inequality with the detection loophole closed. Using the recent theory result of Ref. [17] and the new theory developed in Supplemental Material, Sec. I [18], we provide a sufficient condition for nonsteerability, valid for general POVMs performed on arbitrary two-qubit states with loss, and conclusively show that our state is not steerable in the opposite direction. We further demonstrate the impact of different experimental parameters, which highlights the delicate nature of experimental one-way steering. Although the formalism does not assume it, our experimental states are very close to two-qubit Werner states. Two-qubit Werner states comprise a one-parameter family of states written as $\rho_W = \mu|\Psi^-\rangle\langle\Psi^-| + (1-\mu)/4\mathbf{I}_4$, where $|\Psi^-\rangle = (|01\rangle - |10\rangle)/\sqrt{2}$ is the singlet state and $\mathbf{I}_4$ is the 4×4 identity matrix. These states represent a well-known example of mixed states [22], with their purity determined by the Werner state parameter $\mu \in [0, 1]$.

A number of sources of photonic two-qubit Werner states have been reported in the past [23–27]. Here, we use a new type of photon source, producing high-quality states that have unprecedented fidelities with Werner states.

Werner state source.—Our photonic source of Werner states is based on spontaneous parametric down-conversion (SPDC) with a picosecond pulsed pump laser, producing photon pairs at a telecom wavelength, with the quantum state encoded in the polarization degree of freedom ($|H\rangle \equiv |0\rangle$, $|V\rangle \equiv |1\rangle$, where H and V stand for horizontal and vertical polarization, respectively). It is constructed as an incoherent superposition of a singlet state source and a source of maximally mixed photon pairs. Our design provides high heralding efficiencies and full control of the Werner state parameter μ.

The detailed setup is illustrated in Fig. 2. A 775 nm pulsed laser with variable power and a pulse length of 1 ps acts as the pump for the two individual sources comprising the overall source. After passing through a focusing lens, the pump beam is divided between the two sources with a controllable splitting ratio by using a half-wave plate (HWP) and polarizing beam splitter (PBS).

The singlet state source is based on the design of Ref. [28] and essentially implements a superposition of two SPDC events within a beam displacer interferometer. The pump passes through a HWP that sets its polarization to an equal superposition of H and V components, which are then horizontally split into two beams by the first beam displacer (BD). The next two HWPs act to make the polarizations of both beams H, appropriate for the subsequent down-conversion process, while matching the path lengths of the two beams. The beams then pump the 15-mm-long periodically poled potassium titanyl phosphate (ppKTP) crystal in two places, enabling degenerate type-II SPDC. The second BD separates signal and idler photons vertically, resulting in a total of four down-converted photon beams for the one photon pair. The next three HWPs modify the polarizations of the beams such that the left two beams are H polarized, while the right two beams are V polarized. This allows overlapping the signal photon from the two different down-conversion beams with the third BD, and likewise for the idler photon. A D-shaped mirror separates the propagation directions of the signal and idler photon beams, each of which are collimated, have

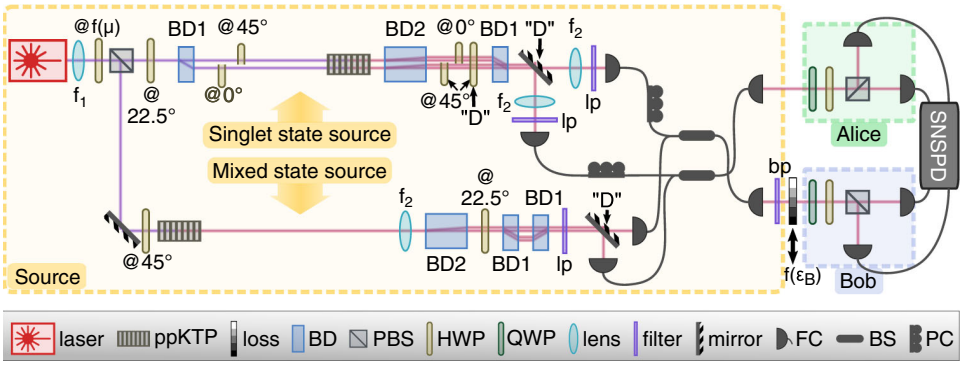

FIG. 2. Experimental setup. As detailed in the main text, the tunable source of telecom-wavelength two-qubit Werner states is constructed as an incoherent superposition of the outputs from a singlet state source and a source of the maximally mixed two-qubit state. After a variable loss in one arm, polarization measurements are carried out in Alice and Bob's stations, enabling quantum state reconstruction and steering tests. Abbreviations: ppKTP, periodically poled potassium titanyl phosphate; BD, (polarizing) beam displacer; PBS, polarizing beam splitter; HWP, half-wave plate; QWP, quarter-wave plate; FC, (single-mode) fiber coupler; BS, (fiber) beam splitter; PC, (fiber) polarization controller; SNSPD, superconducting nanowire single-photon detectors; lp, long pass; bp, bandpass; "*D*," D-shaped element with a horizontal cut that is not apparent from the top view. BD2 implements a vertical beam displacement (see the main text), which is illustrated in the diagram by the slightly separated pairs of beams. For further details about the experimental elements, see Supplemental Material, Sec. III [18].

the pump light filtered out with a long-pass filter, and are coupled into single-mode fiber. To transform the maximally entangled state of $|HH\rangle$ and $|VV\rangle$ to one of $|HV\rangle$ and $|VH\rangle$, a 90° polarization rotation for one of the two photons is implemented with in-fiber polarization controllers, and the phase ϕ of the target state $(|HV\rangle - e^{i\phi}|VH\rangle)/\sqrt{2}$ can be controlled through a slight tilting of the first BD or by adjusting the crystal temperature.

The design of the mixed state source is such that a separable photon pair is created, and then each photon is fully depolarized, yielding the target state $\mathbf{I}_4/4$. The pump beam passes through a ppKTP crystal identical to the one in the entangled state source, creating one H and one V polarized photon, which are collimated with a lens. The two photons are vertically separated into two beams with a BD, and subsequently their polarization is rotated by 45° with a HWP. An imbalanced BD interferometer, in which one polarization component passes straight through and the other component undergoes spatial walk-off twice (in opposite directions), decoheres the polarization of each of the signal and idler photon completely. A long-pass filter discards the pump light, before the propagation directions of the signal and idler beams are separated with a D-shaped mirror and they are fiber coupled.

The two individual sources are mixed using 50:50 fiber beam splitters, which combine the signal photon contributions coming from the two sources, and likewise for the idler photon. This mixing is incoherent, since the path lengths through the two sources are sufficiently different. Finally, a bandpass filter in Bob's arm narrows the biphoton spectrum (see Sec. III in Ref. [18]), which enhances the polarization state quality for the singlet source. By tuning the relative power of the pump in the two individual sources, the parameter μ can be controlled. For a range of relative power values, we perform quantum state tomography of the photon pairs using a combined pump power setting of ~75 mW and determine the fidelities with the closest Werner states, as detailed in Table I. These fidelities are the highest reported values to date.

A further noteworthy feature of our source is its high heralding efficiency. Despite a 50% loss due to the mixing of the two individual sources via 50:50 beam splitters and the additional components in the measurement apparatus, we still obtain typical heralding efficiencies (defined as detected coincidences divided by the detected singles of the opposite arm, also called Klyshko efficiency [29]) of 0.3100 ± 0.0003 and 0.2345 ± 0.0002, for the arm without and with the bandpass filter, respectively. The

TABLE I. Tunability and quality of the experimental quantum state. For six different pump conditions, we determine the Werner state ρ_W with which the experimental state ρ has the highest fidelity. Listed are the parameter μ of the closest Werner state and the corresponding fidelity, defined as $[\mathrm{Tr}(\sqrt{\sqrt{\rho}\rho_W\sqrt{\rho}})]^2$. Uncertainties are obtained from Monte Carlo simulations based on Poisson distributed counts to generate 200 variations on each of the experimental tomography measurement results. The reconstructed density matrices are shown in Supplemental Material, Sec. II [18].

μ	0.9978 ± 0.0003	0.797 ± 0.001	0.603 ± 0.001	0.398 ± 0.002	0.198 ± 0.002	0.007 ± 0.002
State fidelity	0.9981 ± 0.0002	0.9964 ± 0.0004	0.9983 ± 0.0002	0.9985 ± 0.0001	0.9986 ± 0.0001	0.9983 ± 0.0001

high heralding efficiencies are made possible by the choices of the pump beam waist, the detection beam waist, and high-efficiency superconducting nanowire single-photon detectors [30] (see also Sec. III in Ref. [18]).

One-way steering.—To demonstrate one-way steering, we use the same setup as before, with some minor modifications. To add controllable loss, we insert a multi-setting neutral density filter before the detection apparatus in Bob's arm, which lowers his overall heralding efficiency to ε_B. We also increase the total pump power to ~300 mW in order to maintain a sufficiently high signal-to-noise ratio with the attenuated beam against the detector dark counts, which are ~100 per second (see Sec. III in Ref. [18]). As shown in Fig. 3 and explained below, the output of our Werner state source together with the added loss creates one-way steerable states, provided that the values of μ and ε_B are suitably chosen. Note that, in the steering experiment, some of the fidelities with the closest Werner states are lower than the results shown in Table I, but our subsequent analysis is robust, as it makes no assumption of the experimental states being Werner states.

To demonstrate one-way steering, we perform two sets of measurements. The purpose of the first set is to show steering from Alice to Bob. This is done via a steering test with $n = 6$ measurement settings, using a platonic-solid measurement scheme [31]. Detection-loophole-free steering is demonstrated if the correlations of the measurement outcomes are sufficiently large, resulting in a steering parameter that exceeds the $n = 6$ steering bound (the definition of the steering parameter is provided in Supplemental Material, Sec. IV [18]). The bound is a function of Alice's heralding efficiency ε_A, because, in this task, she is the person who is attempting to steer her opponent's state. Our experiment thus necessarily closes the detection efficiency loophole, though we make no claim to close the spacelike-separation loophole.

The purpose of the second set of measurements is to establish nonsteerability from Bob to Alice, for general POVMs. This is achieved via a quantum state tomography, through which our experimental density matrix is reconstructed. Based on the density matrix and Bob's experimentally measured heralding efficiency, we test the criterion for nonsteerability derived in Supplemental Material, Sec. I [18]:

$$N_{\mathrm{POVM}} \leq 1. \tag{1}$$

Here N_{POVM} is defined as

$$N_{\mathrm{POVM}} = \max_{\hat{\mathbf{x}}\in\mathbb{R}^3} \left[(1-3\varepsilon_B)|\mathbf{b}\cdot\hat{\mathbf{x}}| + \frac{3\varepsilon_B}{2}[1+(\mathbf{b}\cdot\hat{\mathbf{x}})^2] + ||T\hat{\mathbf{x}}|| \right], \tag{2}$$

where $\mathbf{b}$ is Bob's local Bloch vector, T is the correlation matrix of the quantum state in its canonical form, and $||\ldots||$ denotes the 2-norm. The maximization is carried out over all unit vectors $\hat{\mathbf{x}}$ in three dimensions. This criterion is stronger than that in Ref. [17], and its derivation (see Supplemental Material, Sec. I [18]) is more rigorous: It ensures nonsteerability from Bob to Alice without restricting Bob's measurements to POVMs on the photonic qubit subspace.

Obtaining a steering parameter in one direction above the steering bound and showing, based on the density matrix and heralding efficiency, that the corresponding quantum

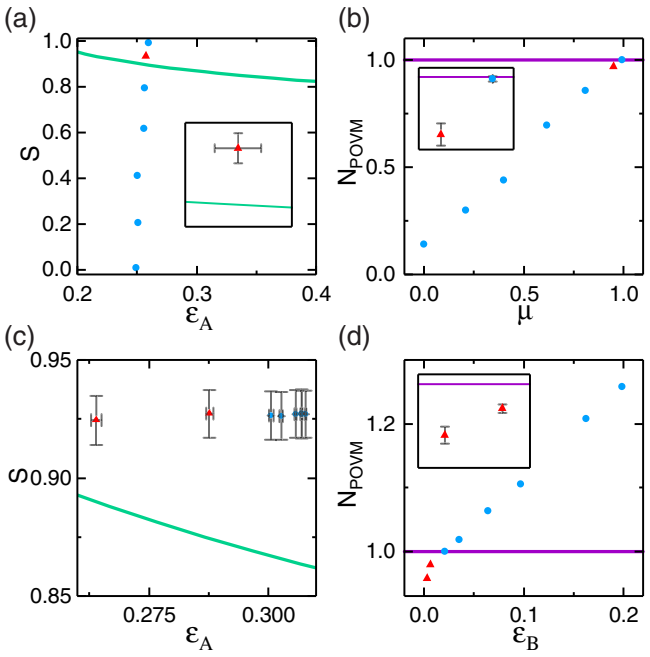

FIG. 3. Experimental demonstration of one-way steering. The upper (lower) panels contain results for a set of states where the effective μ parameter (Bob's heralding efficiency ε_B) is varied. The left panels contain results for a detection-loophole-free steering test for Alice to steer Bob, where the steering parameter S for $n = 6$ measurement settings is plotted against Alice's heralding efficiency ε_A. For any data point above the bound given by the green line, steering from Alice to Bob is demonstrated. The right panels depict results for our sufficient condition for nonsteerability with arbitrary POVMs, and data points below the purple line are conclusively nonsteerable from Bob to Alice. Each data point from one of the left panels corresponds to a point from the right panel, with a pair representing a specific quantum state. Data points in order of increasing S from (a) correspond to the points with increasing μ in (b). Similarly, data points in order of increasing ε_A in (c) correspond to those with increasing ε_B in (d). Uncertainties for the steering parameter are calculated as $\Delta S = \sqrt{\Delta S(\mathrm{systematic})^2 + \Delta S(\mathrm{statistical})^2}$ [31]. The other uncertainties are based on Monte Carlo simulations of the measurement outcomes, using 200 samples of Poisson distributed counts. Where uncertainties are small and error bars would reduce the clarity of the plots, the error bars are not shown. However, the relevant uncertainties are provided in the insets, which enlarge areas of interest. Conclusively one-way steerable states are marked by the red triangles.

state is unsteerable in the opposite direction successfully demonstrates one-way steering. We perform the measurements for two sets of quantum states. In the first set, we keep the loss added by the neutral density filter fixed such that Bob's heralding efficiency is $\varepsilon_B = (2.52 \pm 0.03) \times 10^{-3}$ while varying μ. The results from the steering test are shown in Fig. 3(a), and the results from the corresponding test of the sufficient condition for nonsteerability in the opposite direction are depicted in Fig. 3(b). Of all the μ values shown, only one, marked by the red triangle, is conclusively one-way steerable [steering bound violation from Alice to Bob by 3.8 standard deviations (s.d.) and fulfilment of the sufficient condition for nonsteerability from Bob to Alice with a margin of 5.3 s.d.].

For the second set of quantum states, we keep μ fixed at 0.951 ± 0.004 while varying the loss added by the neutral density filter. The results of the steering test are given in Fig. 3(c), and the results from the corresponding test of the sufficient condition for nonsteerability in the opposite direction are shown in Fig. 3(d). Here, the two states corresponding to the lowest ε_B values are conclusively one-way steerable (steering bound violation by 3.3 and 5.2 s.d. and nonsteerability with margins of 6.0 and 5.6 s.d., respectively). The states with higher ε_B are no longer conclusively nonsteerable from Bob to Alice. The ability to further reduce ε_B is limited for technical reasons only, namely, the decreasing signal-to-noise ratio due to dark counts, which reduces the ideally constant measured heralding efficiency ε_A when the attenuation is very high.

The results highlight that, in practice, demonstrating one-way steering based on two-qubit states with loss requires a balance between (i) having sufficient correlations to observe steering in one direction while (ii) keeping the loss needed to conclude nonsteerability in the opposite direction at a technically feasible level.

Discussion.—Our experiment is based on a two-qubit state with loss. Implementing loss in a quantum information protocol is relatively straightforward. In fact, some amount of loss is generally unavoidable in practice, so, even if the loss were not actively leveraged, an experimental analysis would need to account for it in any case. Therefore, a two-qubit state with loss is well motivated from a practical perspective.

It is worth emphasizing that we establish nonsteerability by checking against our *sufficient* condition for nonsteerability [Eq. (1)]. This condition offers the best currently available method for demonstrating the nonsteerability of general two-qubit states with loss, allowing for general POVMs. However, the condition is not proven to be tight, so it is possible that tighter conditions will be found in the future. For example, it might be possible to show that the necessary and sufficient conditions for steerability coincide for projective measurements and POVMs, which would then make it easier to demonstrate one-way steering. However, the fact that we work with a sufficient condition for nonsteerability means that our results are conclusive now and will remain so, even in the event that tighter conditions are found in the future.

Conclusion.—In this work, we present a new, high-heralding-efficiency photon-pair source that produces quantum states with very large fidelities with two-qubit Werner states and provides full control of the Werner state parameter. We use the source and a new sufficient condition for nonsteerability to achieve a rigorous demonstration of two-qubit one-way steering free of previous limiting assumptions about the experimental quantum state or measurement.

This work was supported by the Australian Research Council (ARC) Centre of Excellence CE110001027 and CE170100012. F. G., T. J. B., and S. W. acknowledge financial support through Australian Government Research Training Program Scholarships. H. C. N. acknowledges support by the Deutsche Forschungsgemeinschaft (DFG) and the European Research Council (ERC) (Consolidator Grant No. 683107/TempoQ).

*g.pryde@griffith.edu.au

[1] H. M. Wiseman, S. J. Jones, and A. C. Doherty, Phys. Rev. Lett. **98**, 140402 (2007).
[2] M. T. Quintino, T. Vértesi, D. Cavalcanti, R. Augusiak, M. Demianowicz, A. Acín, and N. Brunner, Phys. Rev. A **92**, 032107 (2015).
[3] D. J. Saunders, S. J. Jones, H. M. Wiseman, and G. J. Pryde, Nat. Phys. **6**, 845 (2010).
[4] J. Bowles, T. Vértesi, M. T. Quintino, and N. Brunner, Phys. Rev. Lett. **112**, 200402 (2014).
[5] C. Branciard, E. G. Cavalcanti, S. P. Walborn, V. Scarani, and H. M. Wiseman, Phys. Rev. A **85**, 010301(R) (2012).
[6] S. L. W. Midgley, A. J. Ferris, and M. K. Olsen, Phys. Rev. A **81**, 022101 (2010).
[7] V. Händchen, T. Eberle, S. Steinlechner, A. Samblowski, T. Franz, R. F. Werner, and R. Schnabel, Nat. Photonics **6**, 596 (2012).
[8] P. Skrzypczyk, M. Navascués, and D. Cavalcanti, Phys. Rev. Lett. **112**, 180404 (2014).
[9] D. A. Evans and H. M. Wiseman, Phys. Rev. A **90**, 012114 (2014).
[10] S. Wollmann, N. Walk, A. J. Bennet, H. M. Wiseman, and G. J. Pryde, Phys. Rev. Lett. **116**, 160403 (2016).
[11] J. Bowles, F. Hirsch, M. T. Quintino, and N. Brunner, Phys. Rev. A **93**, 022121 (2016).
[12] K. Sun, X. J. Ye, J. S. Xu, X. Y. Xu, J. S. Tang, Y. C. Wu, J. L. Chen, C. F. Li, and G. C. Guo, Phys. Rev. Lett. **116**, 160404 (2016).
[13] S. Rao, X. Hu, L. Li, and J. Xu, J. Phys. B **49**, 225502 (2016).
[14] Y. Xiao, X. J. Ye, K. Sun, J. S. Xu, C. F. Li, and G. C. Guo, Phys. Rev. Lett. **118**, 140404 (2017).
[15] M. K. Olsen, Phys. Rev. Lett. **119**, 160501 (2017).
[16] M. Wang, Z. Qin, and X. Su, Phys. Rev. A **95**, 052311 (2017).
[17] T. J. Baker, S. Wollmann, G. J. Pryde, and H. M. Wiseman, J. Opt. **20**, 034008 (2018).

[18] See Supplemental Material at http://link.aps.org/supplemental/10.1103/PhysRevLett.121.100401, which includes Refs. [19,20], for the derivation of the nonsteerability criterion and more details about the experiment and its analysis.
[19] F. Hirsch, M. T. Quintino, J. Bowles, and N. Brunner, Phys. Rev. Lett. **111**, 160402 (2013).
[20] J. Barrett, Phys. Rev. A **65**, 042302 (2002).
[21] N. A. Peters, T. C. Wei, and P. G. Kwiat, Phys. Rev. A **70**, 052309 (2004).
[22] R. F. Werner, Phys. Rev. A **40**, 4277 (1989).
[23] Y. S. Zhang, Y. F. Huang, C. F. Li, and G. C. Guo, Phys. Rev. A **66**, 062315 (2002).
[24] M. Barbieri, F. De Martini, G. Di Nepi, and P. Mataloni, Phys. Rev. Lett. **92**, 177901 (2004).
[25] T.-J. Liu, C.-Y. Wang, J. Li, and Q. Wang, Europhys. Lett. **119**, 14002 (2017).
[26] K. Sun, X.-J. Ye, Y. Xiao, X.-Y. Xu, Y.-C. Wu, J.-S. Xu, J.-L. Chen, C.-F. Li, and G.-C. Guo, npj Quantum Inf. **4**, 12 (2018).
[27] J. Li, C.-Y. Wang, T.-j. Liu, and Q. Wang, Phys. Rev. A **97**, 032107 (2018).
[28] L. K. Shalm, E. Meyer-Scott, B. G. Christensen, P. Bierhorst, M. A. Wayne, M. J. Stevens, T. Gerrits, S. Glancy, D. R. Hamel, M. S. Allman, K. J. Coakley, S. D. Dyer, C. Hodge, A. E. Lita, V. B. Verma, C. Lambrocco, E. Tortorici, A. L. Migdall, Y. Zhang, and D. R. Kumor *et al.*, Phys. Rev. Lett. **115**, 250402 (2015).
[29] D. N. Klyshko, Sov. J. Quantum Electron. **10**, 1112 (1980).
[30] F. Marsili, V. B. Verma, J. A. Stern, S. Harrington, A. E. Lita, T. Gerrits, I. Vayshenker, B. Baek, M. D. Shaw, R. P. Mirin, and S. W. Nam, Nat. Photonics **7**, 210 (2013).
[31] A. J. Bennet, D. A. Evans, D. J. Saunders, C. Branciard, E. G. Cavalcanti, H. M. Wiseman, and G. J. Pryde, Phys. Rev. X **2**, 031003 (2012).